Stability of IMEX linear multistep methods for ordinary and delay differential equations

Toshiyuki Koto
Graduate School of Information Science
Nagoya University, Nagoya 464-8601, Japan
E-mail : koto@is.nagoya-u.ac.jp

March 28, 2008

Abstract

Stability properties of IMEX (implicit-explicit) linear multistep methods for ordinary and delay differential equations are analyzed on the basis of stability regions defined by using scalar test equations. The analysis is closely related to the stability analysis of the standard linear multistep methods for delay differential equations. A new second-order IMEX method which has approximately the same stability region as that of the IMEX Euler method, the simplest IMEX method of order 1 is proposed. Some numerical results are also presented which show superiority of the new method.

Keywords IMEX methods, stability regions, delay differential equations
MSC 65L06, 65L20

1 Introduction

We consider ordinary differential equations (ODEs) of the form

$$\frac{d\boldsymbol{u}}{dt} = \boldsymbol{f}(t, \boldsymbol{u}(t)) + \boldsymbol{g}(t, \boldsymbol{u}(t)), \tag{1.1}$$

which arise after spatial discretization of time-dependent partial differential equations (PDEs) of reaction-diffusion type or advection-diffusion type. Here, $\boldsymbol{f}$ denotes a stiff term derived from the diffusion term, and $\boldsymbol{g}$ denotes a nonstiff or mildly stiff term from the reaction or advection term. In many applications, $\boldsymbol{f}$ is linear and $\boldsymbol{g}$ is nonlinear. In order to solve such equations efficiently, a special type of numerical method called IMEX (implicit-explicit) method is often used, which is obtained by applying an implicit formula with a good stability property to the $\boldsymbol{f}$ term and an

explicit formula to the $\boldsymbol{g}$ term. One of the simplest examples is the IMEX Euler method (see, e.g., Ref. [8])

$$\boldsymbol{u}_{n+1} = \boldsymbol{u}_n + \Delta t \boldsymbol{f}(t_{n+1},\, \boldsymbol{u}_{n+1}) + \Delta t \boldsymbol{g}(t_n,\, \boldsymbol{u}_n), \tag{1.2}$$

which is obtained by applying the implicit Euler formula to the $\boldsymbol{f}$ term and the explicit Euler formula to the $\boldsymbol{g}$ term. Here, Δt is the stepsize, $t_n = t_0 + n\Delta t$, and $\boldsymbol{u}_n$ denotes an approximate value of $\boldsymbol{u}(t_n)$. This method is of order 1 in accuracy; higher-order IMEX methods have been constructed along the ideas of linear multistep methods or Runge-Kutta methods (see Ref. [10], IV.4, and the references cited therein). In this paper, we discuss IMEX methods of linear multistep type.

An IMEX linear multistep method for the equation (1.1) is represented as

$$\sum_{j=0}^{k} \alpha_j \, \boldsymbol{u}_{n+j} = \Delta t \sum_{j=0}^{k} \beta_j \, \boldsymbol{f}(t_{n+j},\, \boldsymbol{u}_{n+j}) + \Delta t \sum_{j=0}^{k-1} \beta_j^* \, \boldsymbol{g}(t_{n+j},\, \boldsymbol{u}_{n+j}). \tag{1.3}$$

Here, α_j, β_j denote the coefficients of a k-step linear multistep method. The coefficients β_j^* are determined by $\beta_j^* = \beta_j + \beta_k \, \gamma_j$ with the coefficients γ_j of a suitable extrapolation so as to incorporate β_k into the other coefficients. For study of stability of such IMEX methods, Frank, Hundsdorfer & Verwer [6] have proposed

$$\frac{du}{dt} = \lambda u(t) + \mu u(t), \quad \lambda,\, \mu \in \mathbb{C}, \tag{1.4}$$

as a test equation (see Refs. [2, 9, 14, 16, 17] for related studies), where $\lambda u(t)$ and $\mu u(t)$ correspond to the $\boldsymbol{f}$ term and the $\boldsymbol{g}$ term in (1.1), respectively. Application of the method (1.3) to this test equation yields the difference equation

$$\sum_{j=0}^{k} \alpha_j \, u_{n+j} - z \sum_{j=0}^{k} \beta_j \, u_{n+j} - w \sum_{j=0}^{k-1} \beta_j^* \, u_{n+j} = 0, \quad z = \Delta t \, \lambda,\ w = \Delta t \, \mu. \tag{1.5}$$

The stability region S of the IMEX method is defined as a region of the parameters $(z,\, w) = (\Delta t \, \lambda,\, \Delta t \, \mu)$ such that the zero solution of (1.5) is asymptotically stable. We can study stability of the method on the basis of S in the similar manner as in the case of the standard linear multistep methods (see, e.g., Ref. [7], Chapter V). If a specific scheme is given, we can draw a figure of its stability region numerically by the root locus method, which is useful for comparing stability of different methods. But, S is a region in $\mathbb{C}^2$ ($\simeq \mathbb{R}^4$). It is not easy to construct a new scheme by adjusting the parameters α_j, β_j and γ_j so as to enlarge the stability region S.

To overcome this difficulty, we consider, in addition to the equation (1.4), an earlier test equation

$$\frac{du}{dt} = \lambda u(t) + \mu u(t - \tau), \quad \lambda,\, \mu \in \mathbb{C}, \tag{1.6}$$

proposed by Barwell [3] in 1975 for study of stability of numerical method for delay differential equations (DDEs). Here, $\tau > 0$ is a constant delay. When the stepsize Δt is given in the form

$$\Delta t = \frac{\tau}{m} \quad (m \geq 1 : \text{integer}), \tag{1.7}$$

an IMEX method can be applied to DDEs of the form

$$\frac{d\boldsymbol{u}}{dt} = \boldsymbol{f}(t,\, \boldsymbol{u}(t)) + \boldsymbol{g}(t,\, \boldsymbol{u}(t),\, \boldsymbol{u}(t-\tau)). \tag{1.8}$$

Through application of the IMEX method to the test equation (1.6), we can define the so-called P-stability region $S_P \subset \mathbb{C}^2$ so that $S_P \subset S$ (see Section 2 for the definition and Ref. [4] for general theory on stability of numerical methods for DDEs). The P-stability region S_P characterizes a stability property of the IMEX method for DDEs, and it is not difficult, in some cases, to enlarge S_P by making use of similar techniques to those used in the stability analysis of the standard linear multistep methods for DDEs. Enlarge S through enlarging S_P. This is the fundamental idea of the present paper for construction of an IMEX method with large S.

The paper is organized as follows. In Section 2, we state the definitions of the stability and P-stability regions of an IMEX method, and show a theorem which gives a basic relation between the two regions. In Section 3, we describe a technique for analysis of P-stability regions, and construct a second-order method with a superior stability property. In Section 4, we present numerical results which suggest practicality of the new method.

2 Stability regions

We assume that the linear multistep method determined from α_j, β_j is of order $p \geq 1$, and that γ_j satisfy $\varphi(k\Delta t) = \sum_{j=0}^{k-1} \gamma_j\, \varphi(j\Delta t) + \mathcal{O}(\Delta t^p)$ for any sufficiently smooth function $\varphi(t)$. This condition is rewritten as

$$\sum_{j=0}^{k-1} j^q\, \gamma_j = k^q\ , \quad q = 0,\, \ldots,\, p-1. \tag{2.1}$$

For example, in the case $k = p = 2$, from the condition $\gamma_0 + \gamma_1 = 1$, $\gamma_1 = 2$, the coefficients γ_1, γ_0 are uniquely determined as $\gamma_1 = 2$, $\gamma_0 = -1$, which gives a linear extrapolation. In general, when $p = k$, the pair γ_{k-1}, $\ldots$, γ_0 is uniquely determined from (2.1) and satisfies $\zeta^k - (\zeta - 1)^k = \sum_{j=0}^{k-1} \gamma_j\, \zeta^j$. The pair gives a polynomial extrapolation. The condition (2.1) assures that the local error of the method (1.3) is $\mathcal{O}(\Delta t^{p+1})$ (see, e.g., Ref. [10], p.387, Theorem 4.2). If the method is zero-stable, it converges with $\mathcal{O}(\Delta t^p)$.

Introducing the polynomials

$$\rho(\zeta) = \sum_{j=0}^{k} \alpha_j\, \zeta^j, \quad \sigma(\zeta) = \sum_{j=0}^{k} \beta_j\, \zeta^j, \quad \sigma^*(\zeta) = \sum_{j=0}^{k-1} \beta_j^*\, \zeta^j \tag{2.2}$$

and putting

$$\eta(\zeta;\, z) = \rho(\zeta) - z\,\sigma(\zeta), \tag{2.3}$$

we can write the characteristic equation of the difference equation (1.5) in the form

$$\eta(\zeta;\, z) - w\,\sigma^*(\zeta) = 0 \tag{2.4}$$

and represent the stability region S of the method (1.3) as

$$S = \{(z,\, w) \in \mathbb{C}^2 \,:\, (2.4) \implies |\zeta| < 1\}. \tag{2.5}$$

For example, in the case of the IMEX Euler method (1.2), it follows from $\rho(\zeta) = \zeta - 1,\ \sigma(\zeta) = \zeta,\ \sigma^*(\zeta) = 1$ that the characteristic equation is $\zeta - 1 - z\zeta - w = 0$, which is rewritten as $\zeta = (1+w)/(1-z)$. Hence, the stability region is represented as

$$S = \{(z,\, w) \in \mathbb{C}^2 \,:\, |1+w| < |1-z|\,\}. \tag{2.6}$$

The intersection of the stability region S and the z-plane $\{(z,\, 0) \,:\, z \in \mathbb{C}\}$ is identified with the region

$$S_A \,=\, \{z \in \mathbb{C} \,:\, \eta(\zeta;\, z) = 0 \implies |\zeta| < 1\} \tag{2.7}$$

in the complex plane, which corresponds to the standard stability region of the implicit formula. For each $z \in S_A$, we denote by $\mathit{\Gamma}_z$ the set of all w such that (2.4) has a root with $|\zeta| = 1$. This set is a curve in the complex plane represented in the form

$$\mathit{\Gamma}_z \,:\, \frac{\eta(\zeta;\, z)}{\sigma^*(\zeta)}\ ,\quad \zeta = e^{i\theta},\quad 0 \le \theta \le 2\pi, \tag{2.8}$$

which gives (a part of) the boundary of the z-section $S \cap \{(w,\, z) \,:\, w \in \mathbb{C}\}$. For the IMEX Euler method, we have $\eta(\zeta;\, z)/\sigma^*(\zeta) = -1 + (1-z)\zeta$. Hence, $\mathit{\Gamma}_z$ is a circle centered at -1 with radius $|1-z|$ (Fig. 2.1 left). Restricting the variable z onto the real line, we can regard the stability region as a solid figure in $\mathbb{R} \times \mathbb{C} \simeq \mathbb{R}^3$. The right picture of Fig. 2.1 displays a three-dimensional view of S of the IMEX Euler method, a (solid) cone obtained by aligning the disks $|w+1| < |1-z|$ in the z-direction.

A second-order two-step IMEX method defined with BDF2 (two-step BDF, $\alpha_2 = 3/2,\ \alpha_1 = -2,\ \alpha_0 = 1/2,\ \beta_2 = 1,\ \beta_1 = \beta_0 = 0$) and $\beta_1^* = 2,\ \beta_0^* = -1$ ($\gamma_1 = 2,\ \gamma_0 = -1$) is called the IMEX BDF2 method. In the case of this method, $\mathit{\Gamma}_z$ for negative z is a simple closed curve as shown in the left picture of Fig. 2.2. The right picture displays a three-dimensional view of S of the IMEX BDF2 method, which seems contracted in all directions except for the positive real direction, compared with that of IMEX Euler method (Fig. 2.1).

Under the condition (1.7) for the stepsize, an IMEX linear multistep method for the DDE (1.8) is defined by

$$\sum_{j=0}^{k} \alpha_j\, \boldsymbol{u}_{n+j} = \Delta t \sum_{j=0}^{k} \beta_j\, \boldsymbol{f}(t_{n+j},\, \boldsymbol{u}_{n+j}) + \Delta t \sum_{j=0}^{k-1} \beta_j^*\, \boldsymbol{g}(t_{n+j},\, \boldsymbol{u}_{n+j},\, \boldsymbol{u}_{n-m+j}). \tag{2.9}$$

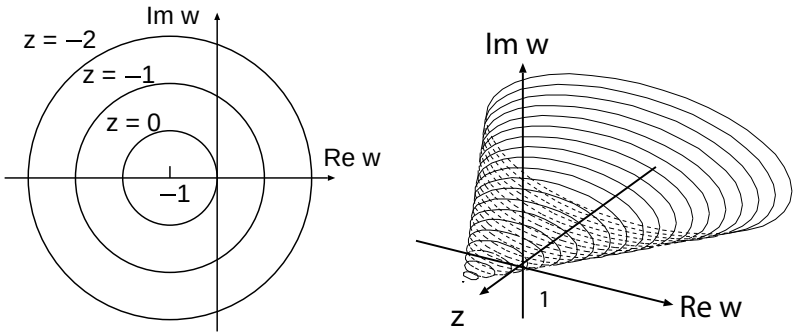

Figure 2.1: Stability region of the IMEX Euler method

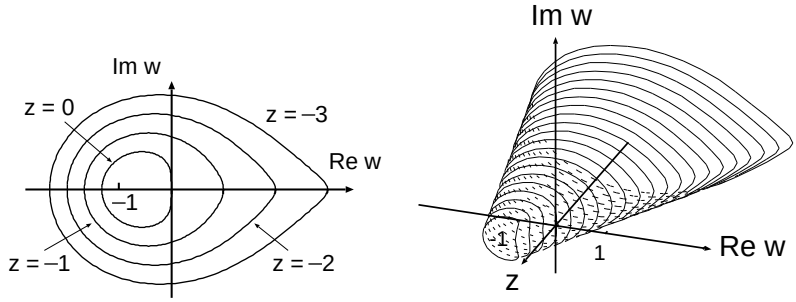

Figure 2.2: Stability region of the IMEX BDF2 method

Application of the method to the test equation (1.6) yields

$$\sum_{j=0}^{k} \alpha_j \, u_{n+j} = z \sum_{j=0}^{k} \beta_j \, u_{n+j} + w \sum_{j=0}^{k-1} \beta_j^* \, u_{n-m+j}, \quad z = \Delta t \lambda, \ w = \Delta t \mu, \tag{2.10}$$

and the characteristic equation of the difference equation (2.10) is written in the form

$$\zeta^m \, \eta(\zeta;\, z) - w \, \sigma^*(\zeta) = 0. \tag{2.11}$$

Using this equation, we define the P-stability region S_P of the IMEX method as

$$S_P = \bigcap_{m \geq 0} S_P^{(m)}, \quad S_P^{(m)} = \{(z,\, w) \in \mathbb{C}^2 \, : \, (2.11) \implies |\zeta| < 1\}. \tag{2.12}$$

By the definition, $S_P \subset S$, and putting

$$\gamma_z = \inf\{|w| \, : \, w \in \mathit{\Gamma}_z \}, \tag{2.13}$$

we can characterize the P-stability region as follows.

Theorem 1. *Assume that the vectors* $(\alpha_0, \, \ldots, \, \alpha_k)$ *and* $(\beta_0, \, \ldots, \, \beta_k)$ *are linearly independent, and consider the following statements:*

(a) $z \in S_A$ *and* $|w| < \gamma_z$; (b) $(z,\, w) \in S_P$; (c) $z \in S_A$ *and* $|w| \leq \gamma_z$.

Then, we have (a) $\implies$ (b) $\implies$ (c).

Proof We first show that (a) $\Longrightarrow$ (b). Let $|\zeta| \geq 1$ and $z \in S_A$. The equation (2.11) is rewritten as

$$\zeta^m = w \, \frac{\sigma^*(\zeta)}{\eta(\zeta;\, z)} \, . \tag{2.14}$$

For any integer $m \geq 0$, the modulus of the left-hand side is greater than or equal to 1. On the other hand, since $z \in S_A$, the right-hand side is holomorphic in $|\zeta| > 1$, and the modulus is less than or equal to

$$|w| \sup_{|\zeta|=1} \left| \frac{\sigma^*(\zeta)}{\eta(\zeta;\, z)} \right| = \frac{|w|}{\gamma_z} \, , \tag{2.15}$$

by the maximal modulus principle. If $|w| < \gamma_z$, this value is less than 1, and hence (2.14), or (2.11) never holds for any $m \geq 0$. This implies that (a) $\Longrightarrow$ (b).

We can prove that (b) $\Longrightarrow$ (c), for example, by making use of a theorem by in 't Hout & Spijker [11] (see also in 't Hout & Spijker [12], Liu & Spijker [15], and Ref. [4], p.310, Lemma 10.2.24). Since $(\alpha_0, \, \ldots \, , \, \alpha_k)$ and $(\beta_0, \, \ldots \, , \, \beta_k)$ are linearly independent, $\eta(\zeta;\, z) \equiv 0$ does not occur for any $z \in \mathbb{C}$. Hence, by Corollary 3 in [11], if $(z, \, w)$ satisfies (b), we have $z \in S_A$ and $|w\sigma(\zeta)| \leq |\eta(\zeta;\, z)|$ for any $|\zeta| = 1$, which clearly implies (c). $\square$

In the case of the IMEX BDF2 method, γ_z is the radius of an inscribed circle in the curve Γ_z (Fig. 2.3 left). Hence, S_P is regarded as a maximal cone included in S and rotationally symmetric with respect to the z-axis (Fig. 2.3 right).

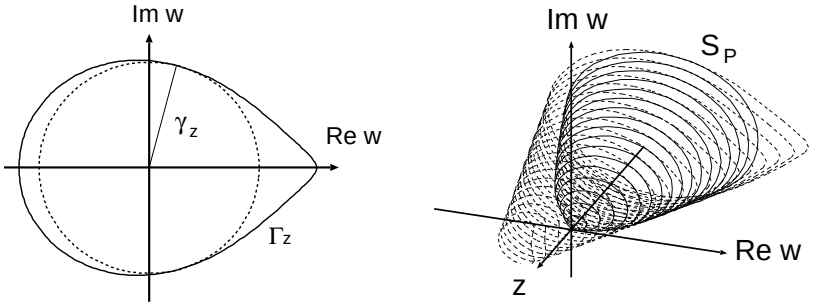

Figure 2.3: P-stability region of the IMEX BDF2 method

In general, it is not difficult to compute an approximate value of γ_z. Let N be a positive integer, and divide the interval $[0, \, 2\pi)$ into N equal parts: $0 = \vartheta_0 < \vartheta_1 < \cdots < \vartheta_k = k\Delta\vartheta < \cdots < \vartheta_N = 2\pi, \ \Delta\vartheta = 2\pi/N$. The curve Γ_z is approximated by

$$\Gamma_{z,\,N} \, : \, \frac{\eta(\zeta_k;\, z)}{\sigma^*(\zeta_k)} \, , \quad \zeta_k = e^{i\vartheta_k}, \quad k = 0, \, \ldots \, , \, N-1, \tag{2.16}$$

and we have

$$\gamma_z = \lim_{N\to\infty} \gamma_{z,\,N}, \quad \gamma_{z,\,N} = \min\{|z| \, : \, z \, \in \, \Gamma_{z,\,N}\}. \tag{2.17}$$

Hence, by taking a sufficiently large N, we can obtain a proper approximate value of γ_z.

3 Analysis of P-stability regions

The stability region of the IMEX BDF2 method is much smaller than that of the IMEX Euler method (2.6). Hereafter, we try to find a second-order IMEX method with larger S through construction of a scheme with larger S_P than that of the IMEX BDF2 method. The following theorem is a fundamental tool for this purpose, which is inspired by Bickart's results [5] in the early 80s concerning stability of the standard linear multistep methods for DDEs.

For $0 < \alpha \leq \pi/2$ and $r \geq 1$, we put

$$D(\alpha) = \{z \in \mathbb{C} \,:\, |\arg(-z)| < \alpha\} \tag{3.1}$$

and

$$\Omega(\alpha,\, r) = \{(z,\, w) \in \mathbb{C}^2 \,:\, z \in D(\alpha),\ r|w| < |z| \sin\theta_\alpha(z)\,\}. \tag{3.2}$$

where $\theta_\alpha(z) = \alpha - |\arg(-z)|$. In the case $\alpha = \pi/2$, they are written as

$$D(\pi/2) = \{z \in \mathbb{C} \,:\, \mathrm{Re}\, z < 0\}\ (= \mathbb{C}^-\,), \tag{3.3}$$

$$\Omega(\pi/2,\, r) = \{(z,\, w) \in \mathbb{C}^2 \,:\, r|w| < -\,\mathrm{Re}\, z\,\}. \tag{3.4}$$

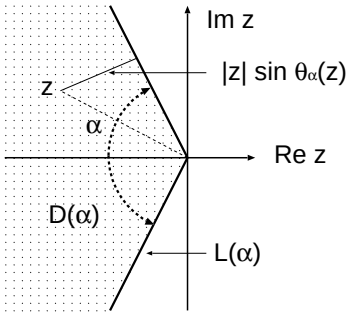

Figure 3.1: The region $D(\alpha)$

Theorem 2. *Let $0 < \alpha \leq \pi/2$, and assume that the implicit formula satisfies the following two conditions:*

(C_1) $S_A \subset D(\alpha)$; (C_2) $\sigma(\zeta) = 0 \Longrightarrow |\zeta| < 1$.

Furthermore, define the curve Γ^* in the complex plane by

$$\Gamma^* \,:\, \frac{\sigma^*(\zeta)}{\sigma(\zeta)}\,, \quad \zeta = e^{i\theta}, \quad 0 \leq \theta \leq 2\pi, \tag{3.5}$$

and put

$$r = \sup\{|w| \,:\, w \in \Gamma^*\,\}. \tag{3.6}$$

Then, we have $r \geq 1$ and

$$S_P \supset \Omega(\alpha,\, r). \tag{3.7}$$

Remark 3. *The condition* (C_1) *is a basic sufficient condition for* $A(\alpha)$*-stability of the implicit formula, and the condition* (C_2) *means the stability at the infinity. In particular, the condition* (C_1) *for* $\alpha = \pi/2$ *corresponds to A-stability, which, together with* (C_2)*, gives L-stability (in terms of Runge-Kutta methods). Moreover, a numerical method for DDEs is said to be P-stable if* $S_P \supset \Omega(\pi/2, 1) = \{|w| < -\mathrm{Re}\, z\}$*. In [5], a method whose P-stability region includes* $\Omega(\alpha, \beta)$ *for some* $0 < \alpha \leq \pi/2$ *and* $\beta \geq 1$ *is called* $P[\alpha, \beta]$*-stable method.*

Proof Since the coefficients γ_j satisfy $\sum_{j=0}^{k-1} \gamma_j = 1$ by (2.1), we have $\sum_{j=0}^{k-1} \beta_j^* = \sum_{j=0}^{k-1} \beta_j + \beta_k \sum_{j=0}^{k-1} \gamma_j = \sum_{j=0}^{k} \beta_j$, which implies $\sigma^*(1)/\sigma(1) = 1$. Hence, the supremum r is greater than or equal to 1.

Assume that $|\zeta| \geq 1$. It follows from (C_1) and (C_2) that $\rho(\zeta)/\sigma(\zeta) - z \neq 0$ for any $z \in D(\alpha)$, which means that $\rho(\zeta)/\sigma(\zeta) \in \mathbb{C} \backslash D(\alpha)$. Hence, we have for $z \in D(\alpha)$

$$\left| \frac{\rho(\zeta)}{\sigma(\zeta)} - z \right| \ \geq \ \inf_{\xi \in L(\alpha)} |\xi - z| \ = \ |z| \sin \theta_\alpha(z) \tag{3.8}$$

(cf. Fig. 3.1), where $L(\alpha)$ is the boundary of $D(\alpha)$, i.e., $L(\alpha) = \{z \in \mathbb{C} : \arg(-z) = \alpha\} \cup \{0\}$. Moreover, the characteristic equation (2.11) is rewritten as

$$\frac{\rho(\zeta)}{\sigma(\zeta)} - z = \zeta^{-m} w \frac{\sigma^*(\zeta)}{\sigma(\zeta)} \ . \tag{3.9}$$

If $r|w| < |z| \sin \theta_\alpha(z)$, this equation does not hold, since the modulus of the left-hand side is greater than or equal to $|z| \sin \theta_\alpha(z)$ by (3.8), and the modulus of the right-hand side is less than $|z| \sin \theta_\alpha(z)$ by the maximal modulus principle. Therefore, we have $S_P \supset \Omega(\alpha, r)$. □

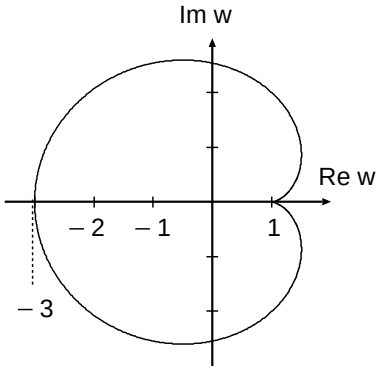

Figure 3.2: Γ^* of the IMEX BDF2 method

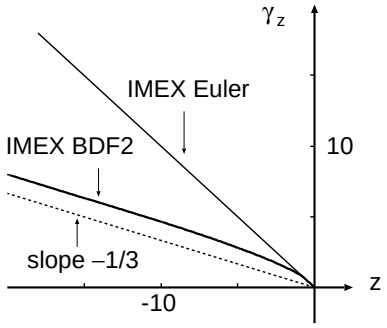

Figure 3.3: γ_z of the IMEX Euler and BDF2 methods

In the case of the IMEX Euler method, since $\sigma(\zeta) = \zeta$ and $\sigma^*(\zeta) = 1$, the curve Γ^* is just the unit circle $\{|w| = 1\}$, and hence $r = 1$. In the case of the IMEX BDF2 method, Γ^* is a simple closed curve displayed in Fig. 3.2. The supremum r

is attained at $w = -3$ as $r = 3$. The implicit Euler formula and BDF2 both satisfy the conditions (C_1) for $\alpha = \pi/2$ and (C_2). By Theorem 2, the P-stability region of the IMEX Euler method includes the region $\{|w| < -\operatorname{Re} z\}$; that of the IMEX BDF2 method includes the region $\{3|w| < -\operatorname{Re} z\}$. Fig. 3.3 displays the functions γ_z for negative z. The graph of γ_z of the IMEX Euler method is the line $-z$ itself; that of the IMEX BDF2 method certainly lies above the line $-z/3$ (dotted line).

A third-order three-step method defined with BDF3 ($\alpha_3 = 11/6$, $\alpha_2 = -3$, $\alpha_1 = 3/2$, $\alpha_0 = -1/3$, $\beta_3 = 1$, $\beta_2 = \beta_1 = \beta_0 = 0$) and $\beta_2^* = 3$, $\beta_1^* = -3$, $\beta_0^* = 1$ ($\gamma_2 = 3$, $\gamma_1 = -3$, $\gamma_0 = 1$) is called the IMEX BDF3 method. As is well known (see, e.g., Ref. [7], V.2), BDF3 satisfies (C_1) for $\alpha = 86.03^\circ$ and (C_2). It is also verified that

$$r = \sup_{|\zeta|=1} \left| \frac{\zeta^3 - (\zeta - 1)^3}{\zeta^3} \right| = 7. \tag{3.10}$$

Hence, $S_P \supset \Omega(86.03^\circ, 7)$. In particular, when $z < 0$, the inequality

$$|w| < \frac{\sin(86.03^\circ)}{7} |z| \ \left(= -0.1425z \right) \tag{3.11}$$

gives a sufficient condition for (z, w) to be included in S_P. Fig. 3.4 displays a comparison of γ_z of the method with the line $-0.1425z$ ($z < 0$), which is indicated by the dotted line. This figure suggests that (3.7) in Theorem 2 is useful for estimate of the size of the P-stability region.

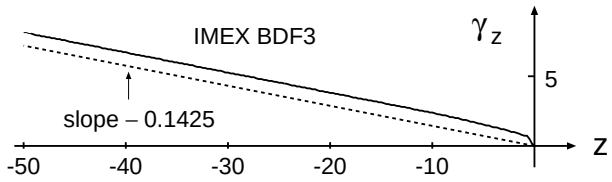

Figure 3.4: γ_z of the IMEX BDF3 method

We look for a second-order method with larger S_P than that of the IMEX BDF2 method in the family of second-order two-step methods. Any second-order two-step linear multistep method is represented in the form

$$\begin{cases} \alpha_2 = a, \quad \alpha_1 = 1 - 2a, \quad \alpha_0 = a - 1 \\ \beta_2 = b, \quad \beta_1 = \dfrac{1}{2} + a - 2b, \quad \beta_0 = \dfrac{1}{2} - a + b, \end{cases} \tag{3.12}$$

with the real parameters a, b, and the conditions (C_1) for $\alpha = \pi/2$ and (C_2) are equivalent to the condition

$$a > \frac{1}{2}, \quad b > \frac{a}{2} \tag{3.13}$$

for a, b (Hairer & Wanner [7], p.249, Exercise V.1.5). Since $\rho(\zeta)$ is written as $\rho(\zeta) = (a\zeta + 1 - a)(\zeta - 1)$, the condition $a > 1/2$ also implies zero-stability of the method. In

particular, the pair $(a,\ b) = (3/2,\ 1)$ corresponding to BDF2 satisfies the condition (3.13). Moreover, it follows from $\gamma_1 = 2$, $\gamma_0 = -1$ that $\beta_1^* = 1/2 + a$, $\beta_1^* = 1/2 - a$, and simple but tiresome computation (cf. Ref. [1] for similar computation) shows that, under the condition (3.13), the supremum r is written as

$$r = \begin{cases} \dfrac{a}{2b-a} & \left(b < \dfrac{a(4a^2-2a+1)}{4a^2+1}\right) \\ \dfrac{4a^2-1}{\sqrt{16b\sqrt{\xi}+\eta}} & \left(b \geq \dfrac{a(4a^2-2a+1)}{4a^2+1}\right) \end{cases}, \tag{3.14}$$

where

$$\begin{aligned} \xi &= 2(2b-2a+1)(b+2a^2-a), \\ \eta &= (4a^2-1)^2 - 8(2a-1)^2 b - 32b^2. \end{aligned}$$

In particular, when $a = b$, this is reduced to

$$r = \frac{2a+1}{2a-1}\ . \tag{3.15}$$

Thus, we can obtain a method satisfying (C_1) for $\alpha = \pi/2$ and (C_2) whose r is sufficiently close to 1, by taking $a = b$ sufficiently large. But, $r = 1$ cannot be attained for the family (3.12). In fact, simple computation shows that the point w on the curve Γ^* takes the modulus $|w| > 1$ in a neighborhood of $w = 1$ (cf. Fig. 3.2) for any a, b.

Taking $a = b = 20$, we obtain $r = 1.0513$ and Γ_z for the corresponding method, displayed in Fig. 3.5. This shows that the stability region of the method is much larger than that of the IMEX BDF2 method and close to that of the IMEX Euler method (Fig. 2.1). We refer to the method as the stabilized second-order method.

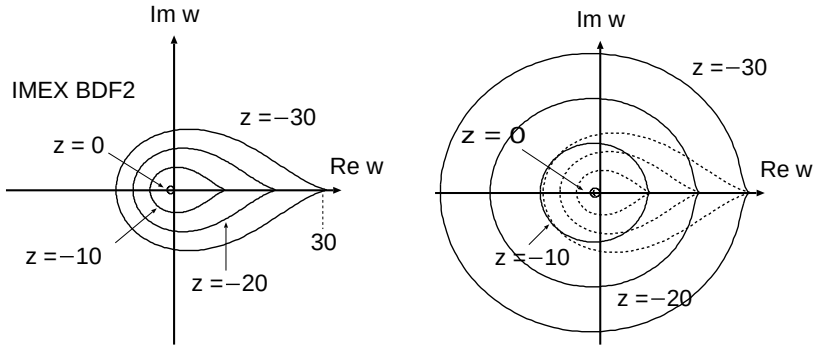

Figure 3.5: Γ_z of the IMEX BDF2 (left) and stabilized method (right)

4 Numerical examples

In this section, we illustrate superiority of the new method using two numerical examples. The first example is the advection-diffusion equation

$$\frac{\partial U}{\partial t} = D\,\frac{\partial^2 U}{\partial x^2} - A\,\frac{\partial U}{\partial x}\ , \quad t \geq 0, \quad 0 \leq x \leq 1, \tag{4.1}$$

with the initial and boundary conditions

$$U(t,\,0) = 1,\ U(t,\,1) = 0,\ t \geq 0, \quad U(0,\,x) = \phi(x),\ 0 \leq x \leq 1. \tag{4.2}$$

Here, D and A are positive constants, and $\phi(x)$ is a given function. It is know (see, e.g., [10], p.84) that this problem has the stationary solution

$$U(t,\,x) = (e^{\frac{A}{D}} - e^{\frac{A}{D}\,x})/(e^{\frac{A}{D}} - 1). \tag{4.3}$$

Fig. 4.1 displays behavior of an exact solution of the equation (4.1).

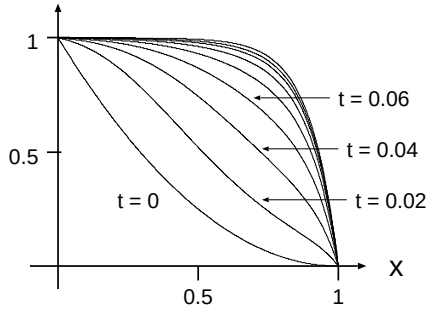

Figure 4.1: Solution of (4.1) for $D = 1,\ A = 10,\ \phi(x) = (1-x)^2$

Let M be a positive integer, $h := 1/M$ and define the mesh points $x_0 = 0 < x_1 < \cdots < x_j = jh < \cdots < x_M = 1$. We use the notation $u^j(t)$ for an approximate function of $U(t,\,x_j)$. By replacing the spatial derivatives with the standard second-order central differences, we obtain the semi-discrete approximation

$$\frac{d\boldsymbol{u}}{dt} = (\boldsymbol{L}\boldsymbol{u}(t) + \boldsymbol{b}) \ - \ \boldsymbol{M}\boldsymbol{u}(t), \tag{4.4}$$

where $\boldsymbol{u}(t) = [u^1(t),\ \ldots,\ u^{M-1}(t)]^T$, $\boldsymbol{b} = [D/h^2 + A/(2h),\,0,\,\ldots,\,0]^T$, and

$$\boldsymbol{L} = \frac{D}{h^2}\begin{bmatrix} -2 & 1 & 0 & \cdots & 0 \\ 1 & -2 & 1 & \cdots & 0 \\ 0 & 1 & -2 & \ddots & 0 \\ \vdots & \vdots & \ddots & \ddots & 1 \\ 0 & \cdots & 0 & 1 & -2 \end{bmatrix},\ \boldsymbol{M} = \frac{A}{2h}\begin{bmatrix} 0 & 1 & 0 & \cdots & 0 \\ -1 & 0 & 1 & \cdots & 0 \\ 0 & -1 & 0 & \ddots & 0 \\ \vdots & \vdots & \ddots & \ddots & 1 \\ 0 & \cdots & 0 & -1 & 0 \end{bmatrix}.$$

For comparison we solved the equation (4.4) using the IMEX Euler, IMEX BDF2 and stabilized second-order methods with various stepsizes of the form $\Delta t = 1/m$, where m is a positive integer. The parameter values are $D = 1,\ C = 10,\ M = 1000$, and the initial function is $\phi(x) = (1-x)^2$. With the two-step methods, we computed starting values at $t = t_1$ using the IMEX Euler scheme. For each method it is observed that the numerical solution tends to a stationary solution if Δt is sufficiently small, but it diverges if Δt is larger than a certain value. For example, in the case of IMEX BDF2 method, the asymptotic property of the numerical solution changes between $m = 53$ and $m = 54$, which can be seen from Figs. 4.2 and 4.3. The former displays the time evolution of the approximate values $u_n^{M/2} \approx U(t_n,\ 1/2)$ at the midpoint of the interval $0 \le x \le 1$ in the cases $m = 53$ and $m = 54$. The latter displays $\log_{10}\ \Lambda_m$ with $\Lambda_m = \max_{5 \le t_n \le 10} |u_n^{M/2}|$ for $50 \le m \le 60$.

Fig. 4.3 displays the results with the IMEX Euler and stabilized methods. We can see that these methods produce stable solutions with much smaller m, i.e., much larger Δt.

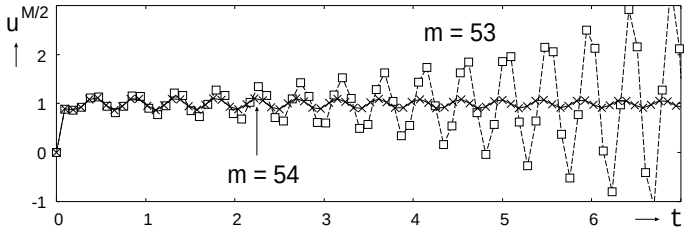

Figure 4.2: Numerical solution of (4.4) by the IMEX BDF2 method

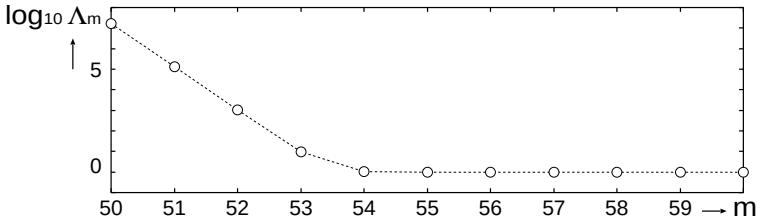

Figure 4.3: Numerical results by the IMEX BDF2 method

Another example is the delay reaction-diffusion equation (cf. Wu [18], p. 220)

$$\frac{\partial U}{\partial t} = D\,\frac{\partial^2 U}{\partial x^2} + \mu U(t-\tau,\ x)[1 + U(t,\ x)^2\,], \quad t \ge 0, \quad 0 \le x \le 1, \tag{4.5}$$

with the initial and boundary conditions

$$U(t,\ 0) = \ U(t,\ 1) = 0,\ t \ge 0, \ \ U(t,\ x) = \phi(t,\ x),\ -\tau \le t \le 0,\ 0 \le x \le 1, \tag{4.6}$$

where τ is a constant delay, D is a positive constant, and μ is a real parameter. By the same spatial discretization as is used for the first example, we obtain the

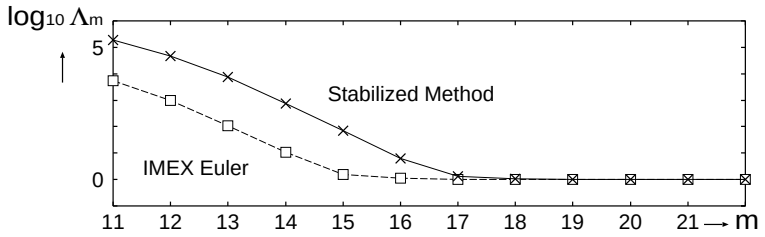

Figure 4.4: Numerical results by the IMEX Euler and stabilized method

semi-discrete approximation

$$\frac{d\boldsymbol{u}}{dt} = \boldsymbol{L}\boldsymbol{u}(t) + g(\boldsymbol{u}(t), \boldsymbol{u}(t-\tau)), \tag{4.7}$$

where $\boldsymbol{L}$ is the same matrix as before and g is an $\mathbb{R}^{M-1}$-valued function whose j-th component is $\mu u^j(t-\tau)\,[\,1+u^j(t)^2\,]$. If $M \geq 3$, all the eigenvalues of $\boldsymbol{L}$ are less than $-8D$; if, in addition, μ satisfies $|\mu| < 8D$, the zero solution of (4.7) is asymptotic stable for any $\tau > 0$ (see, e.g., Koto [13], Section 4). Damped oscillation is typical behavior of the exact solution.

Let $\tau = 1$, $D = 10$, $\mu = -80$ and $M = 1000$. In the case of the IMEX BDF2 method, the asymptotic property of the numerical solution changes with the stepsize $\Delta t = \tau/m\,(= 1/m)$. The numerical solution tends to zero when $m \geq 62$, but it diverges when $m \leq 61$ (Fig. 4.5). Fig. 4.5 displays the time evolution of the approximate values $u_n^{M/2}$ at the midpoint for the initial function $\phi(t,\, x) = x(1-x)$; the IMEX Euler scheme is used for computation of the starting values as before.

On the other hand, with the IMEX Euler and stabilized second-order methods, stable numerical solutions are obtained for any positive integer m. For example, Fig. 4.6 shows the behavior of a solution of (4.7) by the stabilized method with $m = 1$. The same numerical results have been obtained with the IMEX Euler method.

Acknowledgment I would like to thank Yuka Hiraide, a student in a master course of our university for her help with the numerical experiments.

References

[1] Akrivis G, Karakatsani F. Modified implicit-explicit BDF methods for nonlinear parabolic equations. BIT, 2003, 43: 467–483

[2] Ascher U M, Ruuth S J, Wetton B T R. Implicit-explicit methods for time-dependent partial differential equations. SIAM J Numer Anal, 1995, 32: 797–823

[3] Barwell V K. Special stability problems for functional differential equations. BIT, 1975, 15:130–135

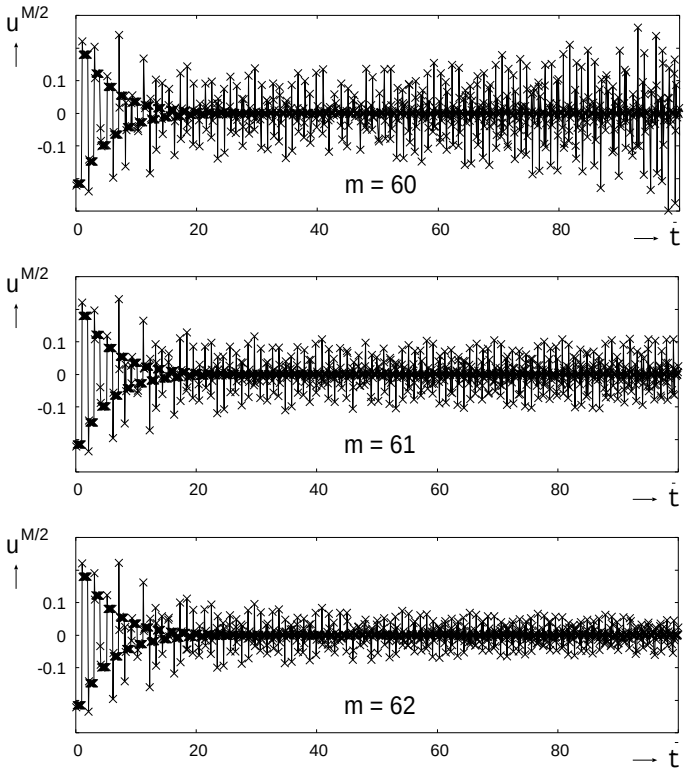

Figure 4.5: Numerical solutions of (4.7) by the IMEX BDF2 method

[4] Bellen A, Zennaro M. Numerical Methods for Delay Differential Equations. New York: The Clarendon Press Oxford University Press, 2003

[5] Bickart T A. P-stable and $P[\alpha, \beta]$-stable integration/interpolation methods in the solution of retarded differential-difference equations. BIT, 1982, 22: 464–476

[6] Frank J, Hundsdorfer W, Verwer J G. On the stability of implicit-explicit multistep methods. Appl Numer Math, 1997, 25: 193–205

[7] E. Hairer, G. Wanner, Solving Ordinary Differential Equations II, Stiff and Differential-Algebraic Problems, second revised ed., Springer-Verlag, Berlin,

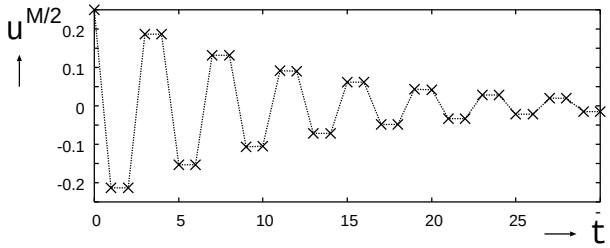

Figure 4.6: Numerical solution of (4.7) by the stabilized method ($m = 1$)

1996.

[8] Hoff D. Stability and convergence of finite difference methods for systems of nonlinear reaction-diffusion equations. SIAM J Numer Anal, 1978, 15: 1161–1177.

[9] Hundsdorfer W, Ruuth S J. IMEX extensions of linear multistep methods with general monotonicity and boundedness properties. J Comput Phys, 2007, 225: 2016–2042

[10] Hundsdorfer W, Verwer J. Numerical Solution of Time-Dependent Advection-Diffusion-Reaction Equations. Berlin: Springer-Verlag, 2003

[11] in 't Hout K J, Spijker M N. The θ-methods in the numerical solution of delay differential equations. In: Strehmel K, ed. Numerical Treatment of Differential Equations. Stuttgart: B. G. Teubner Verlagsgesellschaft mbH, 1991, 61–67

[12] in 't Hout K J, Spijker M N. Stability analysis of numerical methods for delay differential equations. Numer Math, 1991, 59: 807–814

[13] Koto T. Stability of IMEX Runge-Kutta methods for delay differential equations. J Comput Appl Math, 2008, 211: 201–212.

[14] Koto T. IMEX Runge-Kutta schemes for reaction-diffusion equations. J Comput Appl Math, 2008, 215: 182–195

[15] Liu M Z, Spijker M N. The stability of the θ-methods in the numerical solution of delay differential equations. IMA J Numer Anal, 1990, 10: 31–48.

[16] Pareschi L, Russo G. Implicit-explicit Runge-Kutta schemes for stiff systems of differential equations. In: Trigiante D, ed. Recent Trends in Numerical Analysis. Huntington, NY: Nova Science Publishers Inc., 2001, 269–288

[17] Varah J M. Stability restrictions on second order, three level finite difference schemes for parabolic equations. SIAM J. Numer. Anal, 1980,17: 300–309

[18] Wu J. Theory and Applications of Partial Functional-Differential Equations. New York: Springer-Verlag, 1996